JOURNAL OF GEOPHYSICAL RESEARCH, VOL. 115, D06205, doi:10.1029/2009JD011819, 2010

Helical circulations in the typhoon boundary layer

Ryan Ellis[1] and Steven Businger[1]

Received 27 January 2009; revised 7 October 2009; accepted 21 October 2009; published 18 March 2010.

[1] Low-level wind data from the WSR-88D in Guam obtained in Typhoon Dale (1996) and Typhoon Keith (1997) are analyzed for coherent structures. Consistent with the results of previous studies of Atlantic hurricanes, velocity anomalies associated with coherent structures were found in the boundary layer of both storms. A total of 99 cases of coherent structures, also known as roll vortices, were documented during a 6 h evaluation period for each storm. Storm-relative roll location, roll vorticity, asymmetries in the upward and downward momentum fluxes, and signatures of circulations transverse to the mean flow associated with roll circulations were explored. The effects of terrain and convective precipitation systems, such as rainbands, on the occurrence of rolls were investigated. The results support and extend prior findings of roll observations, and can be used to help validate theoretical and numerical models of coherent structures within tropical cyclones. Moreover, the wind variations documented in this study may have application for wave runup and wind damage potential in tropical cyclones.

Citation: Ellis, R., and S. Businger (2010), Helical circulations in the typhoon boundary layer, *J. Geophys. Res.*, *115*, D06205, doi:10.1029/2009JD011819.

1. Introduction

[2] The hurricane boundary layer (HBL) is arguably the most challenging atmospheric environment in which to make accurate observations, yet it is the transfer of energy across the HBL that ultimately helps define the destructive potential of these storms [*Emanuel*, 1986, 1995]. The HBL can be defined as the region of the lower atmosphere that is most directly affected by friction against the ocean surface and the transport of sensible and latent heat across the ocean surface [e.g., *Morrison et al.*, 2005]. A number of recent observational, numerical, and theoretical papers conclusively demonstrated that linearly organized coherent structures are prevalent in HBLs. The observational studies include analyses of land-based Doppler radar studies [*Morrison et al.*, 2005; *Lorsolo et al.*, 2008; *Wurman and Winslow*, 1998; *Wurman et al.*, 2006; *Knupp et al.*, 2006], satellite synthetic aperture radar (SAR) imagery [*Katsaros et al.*, 2002; *Zhang et al.*, 2008], and aircraft penetrations into the boundary layer of Hurricane Isidore [*Zhang et al.*, 2008]. Numerical studies include two-scale boundary layer models [*Ginis et al.*, 2004] and 3-D idealized vortex models [*Nolan*, 2005]. The importance of these structures is in the role they play in the vertical transport of heat, moisture, and momentum. When coherent structures are present, the direct transfer of momentum (and presumably heat and water vapor as well) by these structures across the HBL represents a potentially important contribution to the overall HBL transport of momentum and enthalpy that is not currently included in hurricane models. *Morrison et al.* [2005] estimate that the roll contribution to the momentum flux is about a factor of two larger than what would be calculated using standard turbulence models. This estimate is supported by the theory of *Foster* [2005]. Similar results are found in the aircraft observations of *Zhang et al.* [2008] and the two-scale boundary layer model of *Ginis et al.* [2004]. *Ginis et al.* [2004] modeled the effects of large eddies on the HBL. Their results showed that background wind speed and humidity level control roll formation. After roll formation, the simulations showed a significant increase in 10 m wind speed and surface moisture fluxes, consistent with observations reported by *Lorsolo et al.* [2008]. This may help explain damage patterns observed by *Fujita* [1992] in hurricanes Andrew and Iniki. *Brown and Zeng* [2001] used a two-layer similarity hurricane boundary layer model to simulate roll circulations and show nonlinear roll effects have a large influence on the vertical transport of momentum, moisture, and heat in tropical cyclones.

[3] Observation and theory support the suggestion that HBL-coherent structures can be broadly divided into two categories, (1) streaks, which dominate the lowest layers of the HBL, including the surface and mixed layers [*Wurman and Winslow*, 1998; *Drobinski and Foster*, 2003; and *Lorsolo et al.*, 2008] and (2) roll vortices, which are deeper structures that span all or most of the boundary layer [*Morrison et al.*, 2005; *Foster*, 2005; *Zhang et al.*, 2008]. Near-surface streaks are pervasive features in observations and large-eddy simulations (LESs) of the planetary boundary layer (PBL) in which shear plays an important role in the dynamics [*Deardorff*, 1972; *Moeng and Sullivan*, 1994; *Lin et al.*, 1996; *Glendening*, 1996; *Wurman and Winslow*, 1998]. Streaks have a life cycle of formation and decay of a few tens of minutes and exhibit an average spacing of hundreds of meters. Theoretical predictions that include

[1]Department of Meteorology, University of Hawai'i at Mānoa, Honolulu, Hawaii, USA.

0148-0227/10/2009JD011819

rotation suggest that streaks are the result of nonnormal mode-optimal perturbations [*Drobinski and Foster*, 2003].

[4] By contrast, well-known helical roll vortices have vertical scales of the same order as the depth of the PBL and once they are established can persist for hours or longer. Roll vortices are therefore believed to be the manifestation of normal mode instabilities that reach finite amplitude equilibrium in a modified mean flow [see *Etling and Brown*, 1993 and *Young et al.,* 2002 for reviews].

[5] *Khanna and Brasseur* [1998] and the review of boundary layer linear features by *Young et al.* [2000] discuss how these subkilometer streaks coexist with and are modulated by kilometer-scale rolls. Similarly, *LeMone* [1973] found that the near-surface turbulent energy was modulated by classical kilometer-scale roll vortices. It is likely that the strength of the smaller-scale structures is enhanced underneath the high wind branches of the larger-scale rolls. Of interest is how this affects the strength of the surface stress. We are aware of few studies that have made direct observation of both streaks and rolls coexisting in the same PBL. *Weckwerth et al.* [1997] used lidar and radar data collected in a slightly unstable PBL over land. They found that roll wavelengths were proportional to the depth of the PBL and the roll aspect ratio increased with PBL instability. Moreover, roll orientation was highly correlated with wind direction because no directional shear was required for the formation of rolls. *Lorsolo et al.* [2008] compared data collected by mobile Doppler radars and tower-based in situ measurements in hurricanes. Through spectra analysis they showed that coherent structures in the HBL influence surface winds. These results are consistent with results of *Hogstrom et al.* [2002] who compare measurements of surface layer variances and spectra with theoretical predictions. Their results show that surface layer turbulence is determined by detached eddies that largely originate in the shearing motion immediately above the surface layer, which, in turn, scales with large-scale longitudinal rolls. The focus of this paper is to document roll vortices in the highly sheared rotating HBL of typhoons over the Pacific Ocean using data from the WSR-88D radar located on Guam.

[6] *Browning and Wexler* [1968] developed a technique using a single-Doppler radar that estimates the wind field divergence, translation, and deformation through harmonic analysis of the conventional velocity azimuth display (VAD). Because estimation errors are more pronounced at greater ranges, an optimum scanning procedure was outlined that emphasizes the boundary layer. This led to the study of horizontal roll circulations under varying conditions using single-Doppler and dual-Doppler analysis techniques [*Carbone et al.*, 1985; *Kelly*, 1982; *Christian and Wakimoto*, 1989; *Morrison et al.*, 2005]. *Kelly* [1982] used Doppler radar to explore cloud streets and rolls during lake effect snowstorms over Lake Michigan. *Christian and Wakimoto* [1989] observed cloud streets along the western flank of a ridge in Northeastern Colorado.

[7] *Morrison et al.* [2005] used Level II WSR-88D Doppler radar to observe rolls in data that were collected during three Atlantic hurricanes. They documented that the HBL frequently contains horizontal roll vortices that are approximately aligned along the direction of mean wind. *Morrison et al.* [2005] suggested that the extent of turbulent mixing in the HBL can be taken as the top of the roll circulations documented by analysis of WSR-88D Doppler radar data, and consequently a practical estimate for the extent of the HBL can be determined through the method of radar data analysis described by *Morrison et al.* [2005] and outlined in section 2 of this paper.

[8] While rolls have been previously documented in hurricanes over the Atlantic, this study represents the first time roll vortices have been studied in typhoons. The island of Guam is a good choice for studying roll vortices in tropical cyclones because it is located in an area of the tropical Pacific Ocean commonly traversed by typhoons and because WSR-88D radar data are available for this area.

[9] This study expands on the work presented by *Morrison et al.* [2005] by addressing the vertical component of roll vorticity, asymmetries between the updraft and downdraft portions of the roll circulation, vertical momentum transport, and documenting storm-relative roll locations. In addition, this work illustrates how large-scale convective structures such as rainbands can affect roll circulation and the genesis of new rolls. The effects of terrain on roll circulation are also explored. An increased knowledge of rolls in Pacific tropical cyclones should provide additional insight into the low-level wind variation in tropical cyclones, which hopefully will complement results from the CBLAST experiment that focused on surface fluxes in the hurricane boundary layer [*Black et al.*, 2007; *French et al.*, 2007].

2. Data and Methods

[10] Guam's WSR-88D is located just east of the capital Hagatña (Figure 1). The terrain in the northern part of Guam is characterized by gently rolling mesa-like hills, whereas larger, more rugged mountains characterize most of southern Guam, with elevations ranging from 300 to 400 m above sea level. WSR88D data were available for two typhoons that passed close enough to Guam to observe roll characteristics (Figure 2). These were Typhoon Dale in 1996 and Typhoon Keith in 1997. Although Typhoon Paka was a near direct hit on the island of Guam in 1997, level-II radar data were lost due to a power failure as the storm approached the island.

[11] Typhoon Dale formed at the eastern end of the near-equatorial trough as the result of a westerly wind burst in October of 1996 (Figure 3a). The storm passed 203 km to the south of the Guam radar and resulted in an estimated $3.5 million in damages to the island. Peak gusts on Guam were measured at 38 m s^{-1} at Apra Harbor and the University of Guam in Mangilao. The Guam WSR-88D detected winds of 51 m s^{-1} at heights of 6000–12,000 feet above the surface. The minimum sea level pressure recorded on Guam during the passage of Dale was 987 mb.

[12] Typhoon Keith formed between twin near-equatorial troughs during October of 1997 (Figure 3b). Keith formed in the Marshall Islands and recurved once it passed through the Northern Marianas Islands. The storm passed between the islands of Tinian and Rota, 129 km to the north of the Guam radar, hitting neither island directly. As the storm passed to the north, the Guam WSR-88D observed wind gusts of 72 m s^{-1} in the eyewall. Peak wind gusts observed on Guam were 26–31 m s^{-1}. The Joint Typhoon Warning Center on Nimitz Hill (altitude 183 m) recorded a minimum

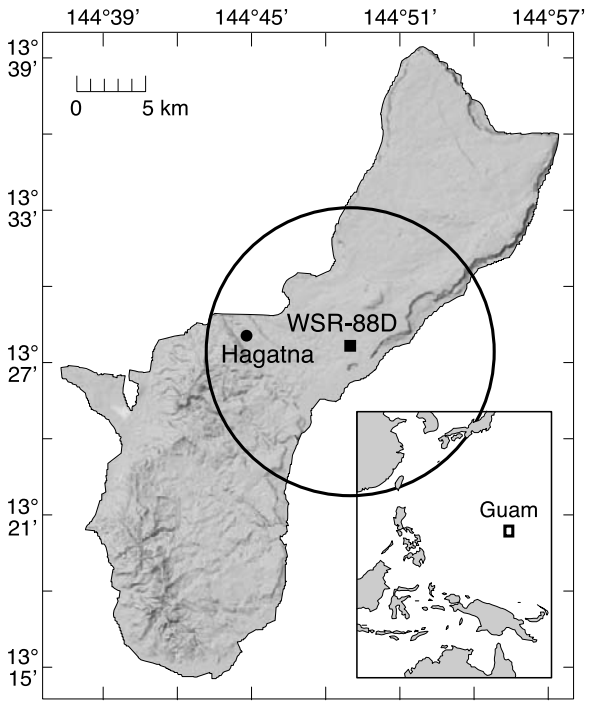

Figure 1. Relief map of Guam showing terrain of the island and location of the WSR-88D radar and 10 km range ring (black square and circle).

pressure of 969 mb, which corresponds to a minimum sea level pressure of 987 mb, identical to that of Typhoon Dale.

[13] Level II data used in this study were collected with the WSR-88D operating in precipitation mode, which completes a volume scan every 6 min. For this study, data were surveyed out to a range of 10 km and only the lowest six elevation angles were used (about 25 s apart) to ensure that the data remain within the boundary layer. At this distance, the beam width is ~160 m, which represents the limit of the vertical and horizontal resolutions perpendicular to the beam at maximum range in this study. The gate-to-gate spacing of the radial velocity data is 250 m. *Crum and Alberty* [1993] provide a more detailed account of the specifications of the WSR-88D. As noted by *Morrison et al.* [2005], the resolution of the DOW, WSR-88D, and the SAR image pixel are comparable, whereas the SMART radar has an angular resolution of 250 m at 10 km range. In each case, the resolution is more than sufficient to resolve the helical rolls described in this paper. Features with a wavelength less than about 320 m are not resolved at the maximum range of 10 km in the WSR-88D data, but these shorter wavelengths can be resolved closer to the radar. The amplitudes of features with wavelengths in the 400–600 m range are well resolved at the 5-range where many of the rolls were identified [*Carbone et al.*, 1985].

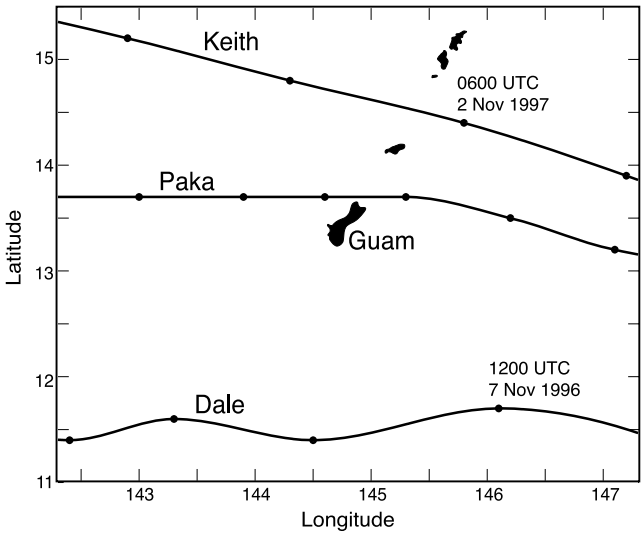

Figure 2. Map of Guam showing best track data for Typhoons Dale (1996), Keith (1997), and Paka (1997) plotted every 6 h (black dots).

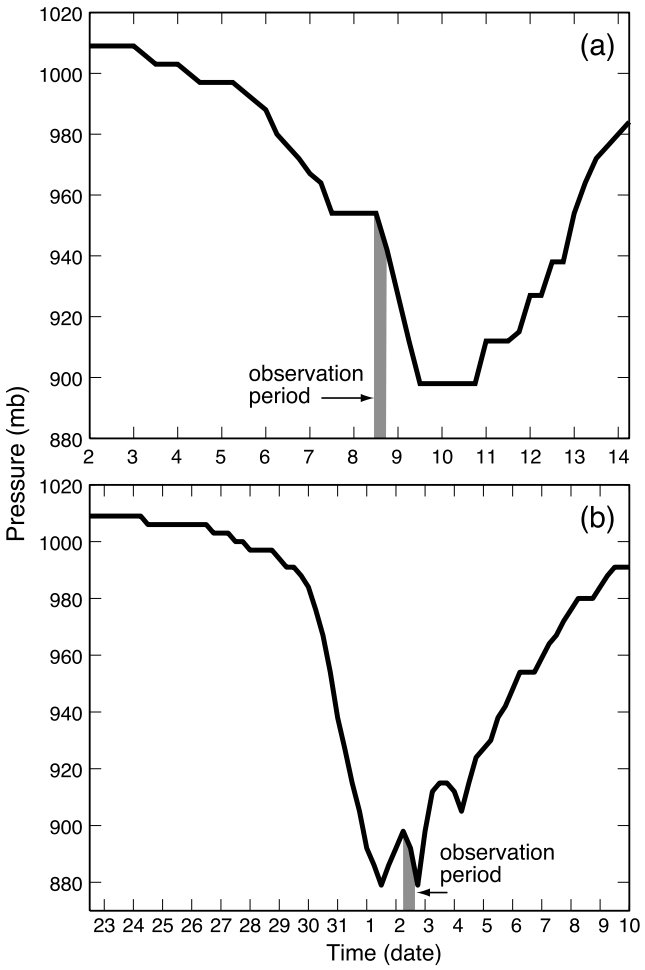

Figure 3. Best track minimum sea level pressure trace for (a) Typhoon Dale and (b) Typhoon Keith with observation period highlighted in gray.

[14] To track potential roll vortices using the WSR-88D, a residual velocity field was created for each elevation angle using a VAD analysis (Figure 4). The residual velocity field was obtained by subtracting the Doppler radial velocity from the first harmonic of the VAD-derived velocity in each radial band. Although the single-Doppler analysis does not provide the ability to obtain all the three components of the roll circulation at once, the alignment of the linear anomaly

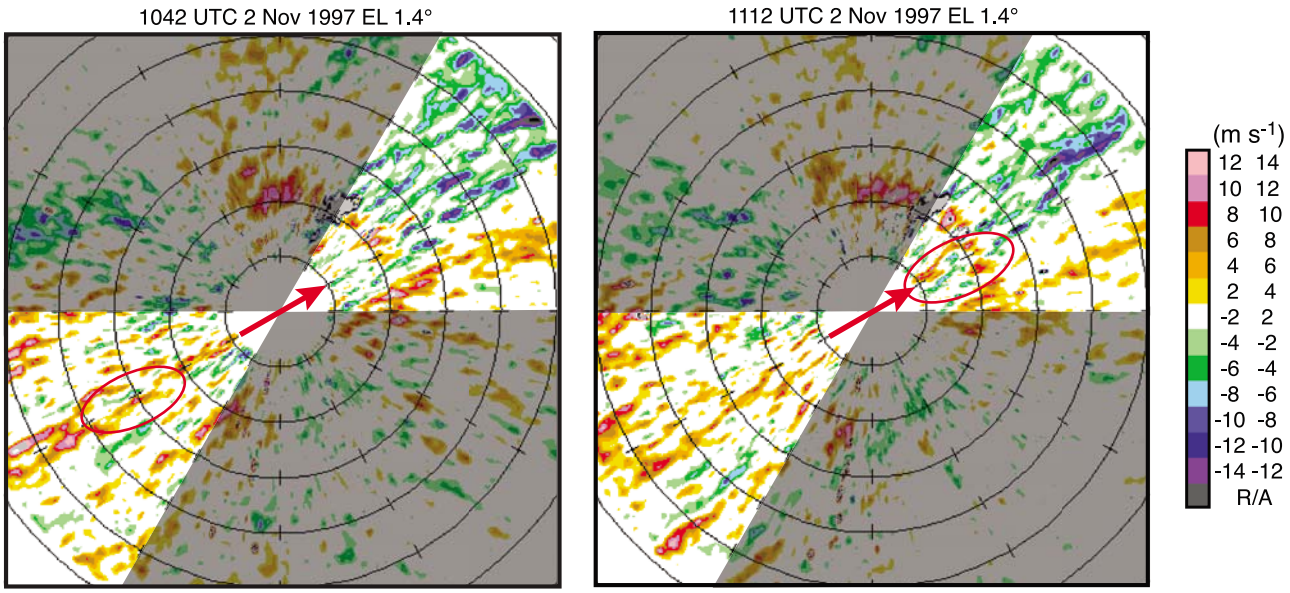

Figure 4. Evidence of roll circulations (red ellipses) aligned along the mean wind direction (red arrow) in successive radar residual velocity volume scans at the 1.4° elevation angle on 2 November 1997. The regions outside a threshold ±30° of the direction of the mean wind are shaded.

features relative to the orientation of the wind can be discerned [*Morrison et al.*, 2005]. Moreover, as the radar beam rotates perpendicular to the wind direction, residuals associated with the crosswise component of the helical circulation can be resolved, as will be discussed in section 3. The only assumption made in this analysis is that the HBL rolls have a life cycle that is long compared with the scan time of the radar. The data confirm that this is the case and fleeting smaller streaks associated with optimal mode instability are excluded from the analysis.

[15] Once the residual velocity field was acquired, a threshold of ±3 m s^{-1} was applied to the field to facilitate the identification of larger coherent structures and eliminate ground clutter. The threshold helps focus the analysis on larger scale roll circulations that are well resolved by the radar data. The residual velocity fields were then examined for pairs of adjacent positive and negative velocity anomalies. The magnitudes of residuals are usually largest within 15° of the mean typhoon boundary layer (TBL) wind direction because of the geometry of the radar velocity data and the action of the rolls in the vertical transport of momentum [*Morrison et al.*, 2005]. Areas that fall within ± 30° of the mean wind direction were the areas of the WSR-88D radar scan that were closely inspected for evidence of roll circulations (Figure 4). To ensure that an observed anomaly pair is indeed a roll circulation, it was tracked in successive scans that occurred about 25 s apart (Figure 5). If the structure was preserved over two successive scans, it was classified as a roll and analyzed. This defines an individual roll case for this study. Rolls were tracked until they ceased to exist within the residual velocity field or until they exited the 10 km range of study.

[16] A variety of characteristics were documented in order to better understand the physical properties associated with roll vortices and their environment. The time and location that a roll occurs within the plan position indicator (PPI) was recorded. The roll location was mapped relative to the storm center using best-track data to estimate the cyclone

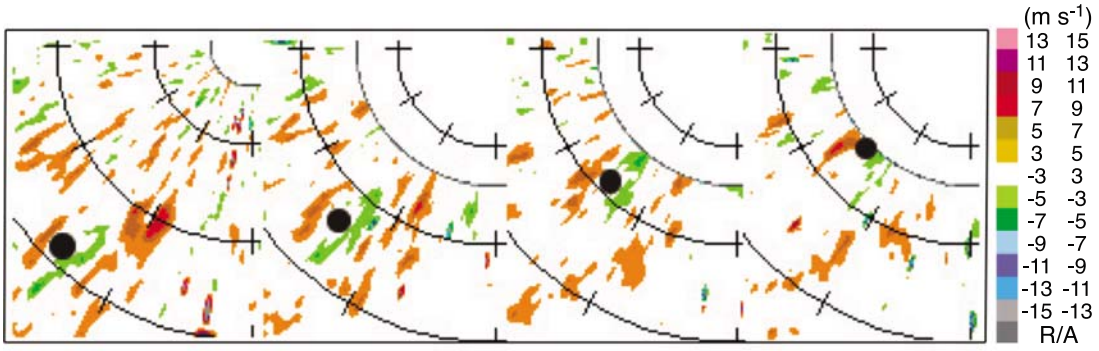

Figure 5. A roll circulation is tracked from the Guam WSR-88D during Typhoon Keith. Each frame is about 25 s apart at subsequent higher elevation angles. Range rings are 2 km apart with hatches representing 30° swaths. Ring without hatches represents the beginning range of observations.

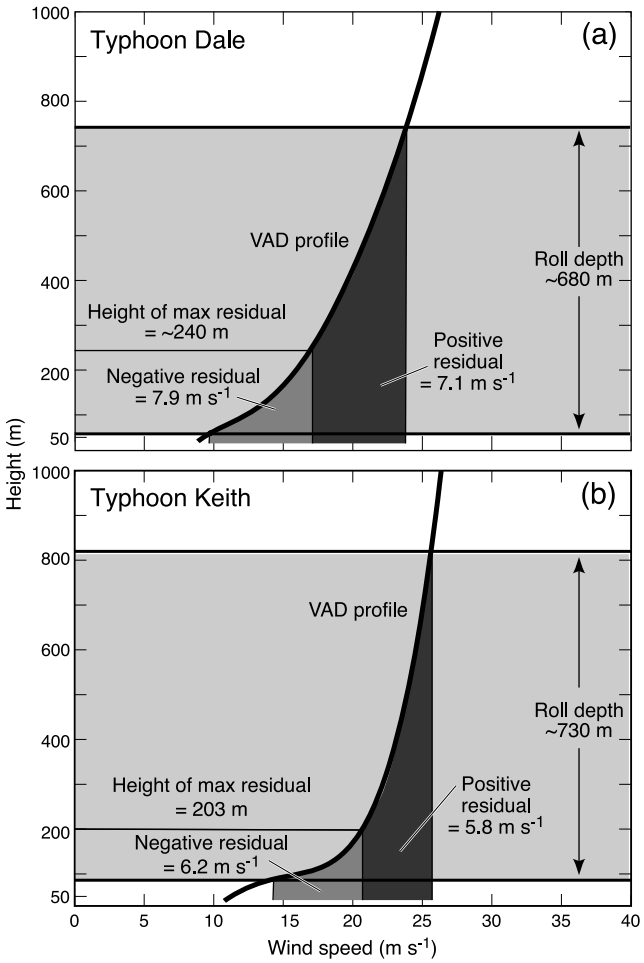

Figure 6. Average VAD profiles over the 6 h observation period for (a) Typhoon Dale and (b) Typhoon Keith. Light gray shading indicates average depth of the boundary layer rolls.

position. The elevation angle at which the roll was first observed was recorded along with range from the radar. The range of the roll observation was measured from the center of the residual velocity couplet to the center of the radar. The height of the observation was then derived from this information.

[17] For each roll documented in the residual velocity field, there is a positive and a negative radial velocity anomaly (relative to the radar) associated with the roll circulation. For the purpose of this study, positive and negative velocity anomalies (relative to the roll) refer to the along wind variation.

[18] The orientation of the roll with respect to the mean typhoon boundary layer wind was computed by measuring the azimuthal angle in degrees between the VAD wind direction and the orientation of the long axis of the roll. This direction is not necessarily the direction of the roll propagation or the direction of the low-level mean wind, as documented in prior studies [*Lorsolo et al.*, 2008].

[19] The distance between the positive and negative anomalies in the residual velocity field represents half of the wavelength of the roll circulation. This distance was measured from the center of the maximum positive residual velocity observation to the center of the maximum negative residual velocity observation in each roll case. The vertical component of vorticity was calculated for each roll by subtracting the negative residual velocity from the positive residual velocity and dividing by half the wavelength, thereby providing an estimate of the magnitude of the positive vorticity.

[20] A Fourier analysis of the VAD was employed to construct wind profiles from the Doppler radar data [*Browning and Wexler*, 1968]. Wind speed and direction estimates were taken from 20 radial bands at 250 m resolution between 5.00 and 9.75 km for each elevation angle [*Marks et al.*, 1999]. This approach provides for estimates every about 25 m up to a height of about 3.4 km, starting at about 100 m above ground level [*Morrison et al.*, 2005]. The VAD wind profiles were constructed throughout the passage of the tropical cyclone and were used to help determine roll depth, aspect ratio, and momentum flux. Wind speed values that make up VAD profiles are averages over the area of each scan rather than values of wind speed at an individual point, and need to be considered when comparing VAD-generated results with conventional observations.

[21] The depth of a typhoon boundary layer roll was estimated through the use of the residual velocity field and the tangential component of the VAD wind profile. The assumption is that the roll circulation transports higher momentum air downward and lower momentum air upward from the level that the maximum residual velocity is observed in the VAD wind profile. Therefore, the depth of the roll is estimated by matching positive and negative velocities to the mean tangential VAD wind profile to determine the top and bottom of the roll circulation (Figure 6). After estimating the depth of the roll, an aspect ratio was computed by dividing the wavelength of the roll by its depth. On the basis of the definition of the aspect ratio, a roll of equal width and height will have an aspect ratio of 2:1.

[22] Mixing length theory, on the basis of principles developed by Prandtl, was used to estimate vertical velocity in roll circulations [*Morrison et al.*, 2005]. The mixing length theory assumes that turbulence is generated mechanically and so it is only valid in statically neutral situations. The theory also assumes linear gradients of wind and moisture. In the real atmosphere, these gradients are likely to remain linear only over small distances [*Stull*, 1988]. Mixing length theory states that

$$u' = -\left(\frac{\partial \overline{U}}{\partial z}\right) z' \text{ and } w' = k \left|\frac{\partial \overline{U}}{\partial z}\right| z'.$$

In the above equations, k is the von Kármán constant ($k = 0.4$), $\partial \overline{U}/\partial z$ is the magnitude of the shear over the depth of the roll, and z' is the depth of the boundary layer roll circulation; u' and w' represent the horizontal and vertical velocity perturbations induced by the roll, respectively. In cases where $\partial \overline{U}/\partial z > 0$, $w' = -ku'$ and when $\partial \overline{U}/\partial z < 0$, mixing length theory states that $w' = ku'$. For the purpose of this study, u' is the positive or negative residual and w' represents the corresponding updraft or downdraft velocity of the roll circulation. In each roll case, the updraft portion of the roll circulation is associated with the negative horizontal

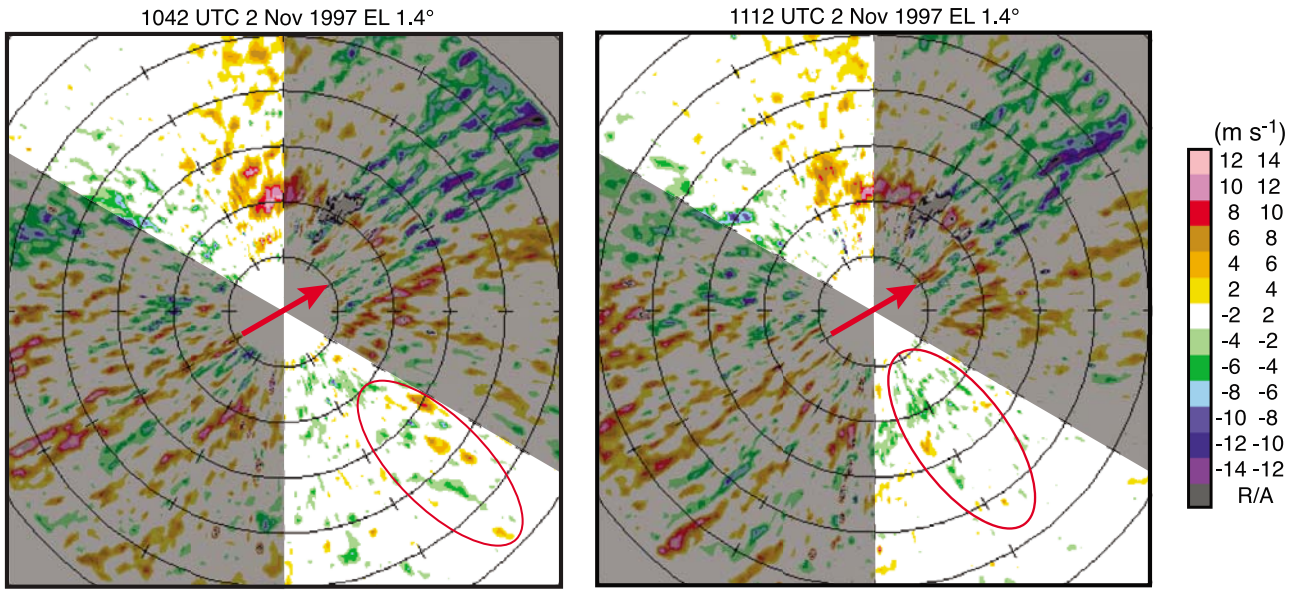

Figure 7. Evidence of transverse circulation (inside red circles) detected normal to the mean wind direction (red arrow) in successive radar scans on 2 November 1997. The region is outside the threshold ±30° of the direction perpendicular to the mean wind is shaded.

velocity anomaly and the downdraft is associated with the positive residual velocity anomaly.

[23] The vertical velocity fluctuations from the mixing length approach were used in conjunction with the horizontal velocity fluctuations obtained from the residual velocity field to estimate momentum flux associated with the updraft and downdraft portions of the roll circulation using the equation $F_m = \overline{u'w'}$. Calculating momentum flux for updraft and downdrafts within the roll circulation is useful in gauging the direct vertical transport of momentum by updrafts and downdrafts in rolls.

[24] The momentum flux associated with rolls was also calculated using an areal average assuming that the flux varied across the roll and is roughly sinusoidal

$$\int \frac{\overline{u'w'}}{l} dl.$$

The equation for the areal-averaged momentum flux integrates the flux with respect to a length equal to one half of the wavelength of the roll to quantify the vertical transport of momentum by the entire roll circulation. The flux has a maximum in the updraft and downdraft portions of the roll and tends to zero in between [*Morrison et al.*, 2005].

[25] It has been suggested that rainbands and other convective elements disrupt the roll circulation [*Morrison et al.*, 2005]. To evaluate this, a rainband case was examined from Typhoon Keith. Reflectivity during and after the passage of the rainband was compared with the corresponding residual velocity fields obtained from the WSR-88D. This information was used to approximate how much of the evaluated area is actually covered by roll vortices in the two situations.

[26] To study how topography and changes in roughness effected the roll circulation, the fetch was classified as either over sea, over flat land, or over mountainous terrain. The number of rolls per hour was then compared with the average wind direction and fetch type in both Typhoon Dale and Typhoon Keith.

[27] The flow perpendicular to the mean wind direction was analyzed in Typhoon Keith for evidence of roll structures. Typhoon Keith was chosen for this part of the study because it passed closer to Guam and yielded twice as many along-flow cases of roll vortices than Typhoon Dale. The goal of this analysis was to be able to detect evidence of

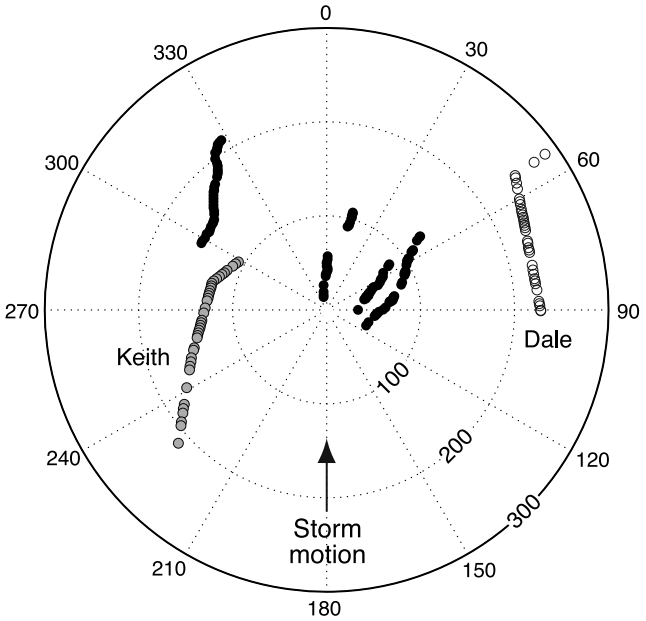

Figure 8. Storm-relative roll locations for Dale (white) and Keith (gray) compared to roll locations observed by *Morrison et al.* [2005] (black). Zero degree indicates the direction of storm motion.

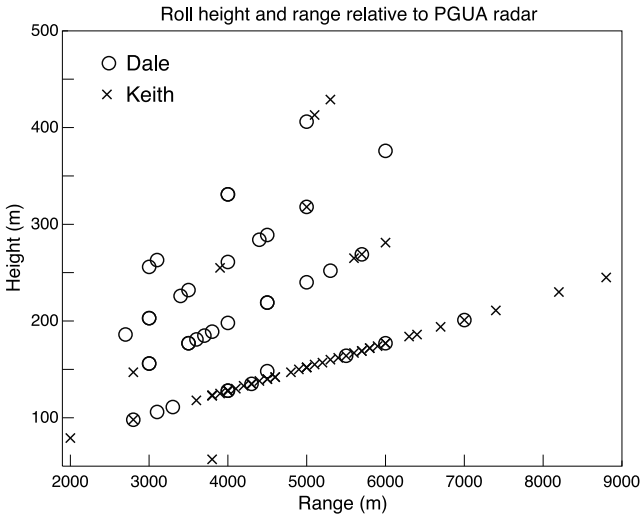

Figure 9. Height and range of maximum anomalies observed by the WSR-88D radar in Typhoon Dale (circle) and Typhoon Keith (cross). Note the vertical axis has been stretched.

the convergence and divergence that is present at the base or the top of the roll circulation. These transverse circulations are the components of the overturning circulation flowing perpendicular to the mean wind. Linear patterns of alternating positive and negative radial velocities were documented normal to the mean flow (Figure 7). For a transverse circulation to be documented, at least one radar observation of converging and one observation of diverging winds have to be present perpendicular to the mean flow. Because the residual velocities in the v direction tended to be smaller than those in the u direction, the threshold of ± 3 m s^{-1} was reduced to ± 2 m s^{-1} to better identify coherent structures while still reducing the amount of noise in the data. Evidence of transverse circulations tended to fall within about $\pm 15^{\circ}$ of the direction perpendicular to the mean wind.

3. Results

[28] Thirty-nine roll vortices were observed by the Guam WSR-88D as Typhoon Dale passed about 200 km to the south of the island during a 6 h window from 1100 to 1700 UTC on 7 November 1996. Sixty rolls were detected as Typhoon Keith passed about 130 km to the north of Guam during the period from 0800 to 1400 UTC on 2 November 1997. In total, 678 PPI scans were analyzed; 339 PPI scans for Typhoon Dale and 339 PPI scans for Typhoon Keith.

[29] Rolls in both storms were found at distances of 100–300 km from the storm center (Figure 8). All rolls were mapped relative to the storm center along with those documented by *Morrison et al.* [2005]. The combined data

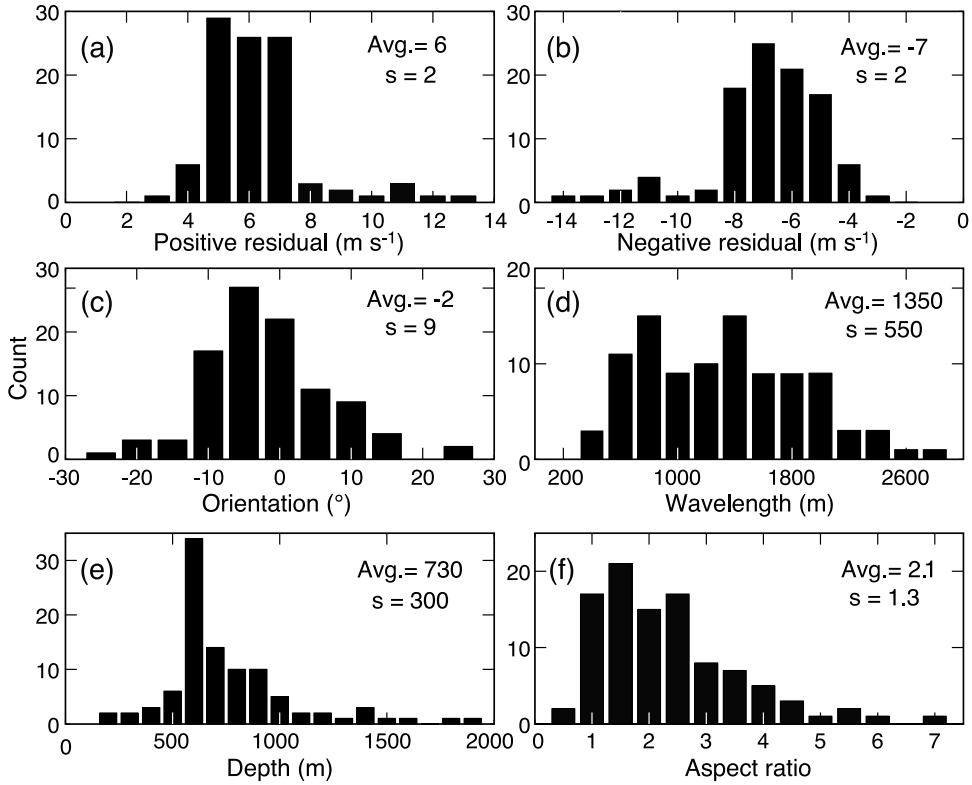

Figure 10. (a) Histogram of positive horizontal wind anomalies (faster than the mean wind speed), (b) negative horizontal wind anomalies (slower than the mean wind speed), (c) roll orientation relative to the mean wind direction, (d) wavelength, (e) depth, and (f) aspect ratio for all rolls found in Typhoons Dale and Keith; s is the standard deviation.

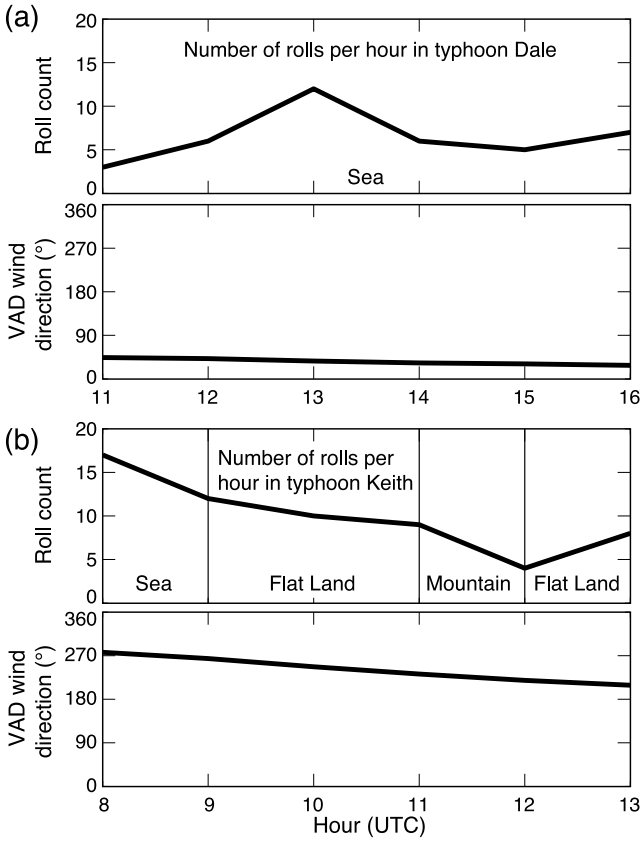

Figure 11. Roll cases observed per hour and VAD wind direction in (a) Typhoon Dale and (b) Typhoon Keith. Fetch type for given wind direction is labeled.

from both studies suggest that roll development occurs both on the leading and trailing sides of tropical cyclones.

[30] The height and range of the greatest anomalies in the residual radar scans were charted (Figure 9). The greatest amount of roll activity was found at heights of about 100–200 m. This activity was dominant along the 1.4° elevation angle, at a range of 3000–6000 m from the radar. Roll activity decreased with increasing elevation angle and height.

[31] The statistics associated with a number of physical properties that help characterize the roll vortices were assembled (Figure 10). Positive residual velocities averaged about 6 m s^{-1} for both storms combined, with a standard deviation of 2 m s^{-1}. Negative residual velocities averaged about −7 m s^{-1} with a standard deviation of 2 m s^{-1}. Roll orientation is defined with respect to the direction of the mean wind, with negative values oriented to the left of the mean wind and positive values oriented to the right of the mean wind. On average rolls were oriented about −2° with a standard deviation of about 9° (Figure 10c). Orientation exhibited nearly a Gaussian distribution, rather than a lognormal distribution, which better characterized the other distributions. Orientation was to the left of the mean wind in 64 of the 99 rolls observed. The average wavelength observed was about 1350 m with a standard deviation of about 550 m (Figure 10d).

[32] Velocity azimuth display wind profiles were calculated for each roll event. The average VAD profile is used to estimate the depth of the average roll circulation (Figure 6). Using this approach, the average roll depth was estimated to be about 680 m in Typhoon Dale (Figure 6a) and about 730 m in Typhoon Keith (Figure 6b). Instead of first averaging the VAD profiles and using average values of the positive and negative residuals to determine the average roll depth, each individual roll depth can be evaluated using the same method as above with the specific VAD profile corresponding to the time of the roll observation, applying the positive and negative residual velocities from each observed roll case. Using this method, the average roll depth was about 730 m with a standard deviation of about 300 m (Figure 10e). Roll aspect ratios for both storms averaged about 2.2 with a standard deviation of about 1.3 (Figure 10f). These aspect ratios show that the observed rolls are roughly as wide as than they are deep.

[33] A comparison of roll count versus the average wind direction was undertaken to find out if the difference in fetch and associated surface roughness affected roll occurrence (Figure 11). Flow approaching the radar in Typhoon Dale was consistently from the northeast throughout the observation period. Terrain in this direction is lower in elevation and less rugged. Roll observations in Typhoon Dale were less variable. A maximum at 1300 UTC coincides with the closest approach of Typhoon Dale to the Guam radar. As Typhoon Keith passed to the north of Guam, the flow approaching the radar first comes from the west, passing over a small amount of land with minimal terrain (Figure 1). As the average wind direction shifted to the southwest, the distance from the radar to the coastline increased. The terrain in this direction is more rugged, reaching elevations above 1000 ft. During this period, the number of rolls documented decreased about 75% from 17 cases observed down to four cases observed. When the average wind direction changed to the south, on the opposite side of the ridge, roll activity increased from four to eight cases.

[34] The horizontal velocity anomalies found in the residual velocity fields were used to estimate the updraft and downdraft wind speeds within the roll vortices through application of mixing length theory [*Morrison et al.*, 2005]. Positive residuals are related to the downdraft portion of the rolls and responsible for downward momentum transport, and the negative residuals correspond to the updraft portion of the roll circulation and thus upward transport of momentum. On average, the updrafts of the roll vortices were slightly stronger than the downdrafts (Figure 12a). Updrafts averaged about 3 m s^{-1} with a standard deviation of about 1 m s^{-1} and downdrafts averaged about −3 m s^{-1} with a standard deviation of about 1 m s^{-1}. Vertical velocity estimates (see section 2) allow for the calculation of the momentum flux. The average value for downward momentum flux specifically associated with the downdraft portion of the roll circulation in Typhoons Dale and Keith was −17 m^2 s^{-2} with a standard deviation of about 10 m^2 s^{-2}. Upward momentum flux associated specifically with the updraft portion of the roll circulation was 20 m^2 s^{-2} with a standard deviation of about 12 m^2 s^{-2}. Estimations of areal-averaged momentum flux over the entire roll circulation averaged about 9 m^2 s^{-2} with a standard deviation of about 5 m^2 s^{-2}. Results shown in Figure 12 were consistent with the findings of *Morrison et al.* [2005] (Table 1).

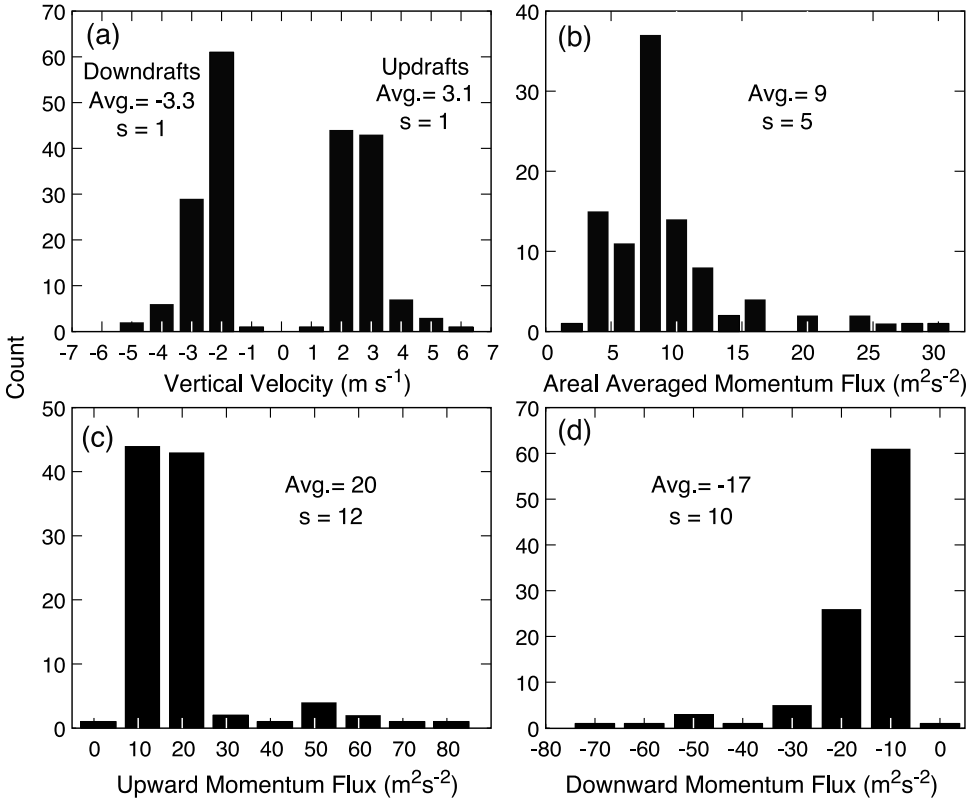

Figure 12. (a) Histogram of estimated updrafts and downdrafts, (b) areal-averaged momentum flux, (c) upward, and (d) downward momentum flux in roll vortices in Typhoons Dale and Keith; *s* is the standard deviation.

[35] *Morrison et al.* [2005] suggested that circulations associated with large convective features within the hurricane, such as rainbands, tend to deter the genesis of roll vortices. During Typhoon Keith, a rainband passed by the Guam WSR-88D (Figure 13a). Thirty minutes after the passage of the feature, the radar recorded low-reflectivity values (Figure 13b).

[36] The corresponding residual velocity scans (Figures 13c and 13d) were inspected for evidence of roll circulations. Of the area that falls within 30° of the mean wind, about 60% is covered with signatures associated with roll circulations in the nonrainband case (Figure 13d). The area of the radar scan covered by rolls falls to about 10% in the rainband case (Figure 12c), suggesting that convective activity suppresses the genesis and/or maintenance of roll vortices.

[37] Evidence of roll circulation perpendicular to the mean flow was examined in Typhoon Keith. The results yielded 25 cases in which anomalies perpendicular to the mean flow were detected by the WSR-88D (e.g., Figure 7). Radial wind couplets highlighting areas of convergence were compared with those highlighting areas of divergence. Normal flow cases showed that areas of convergence were similar, but slightly stronger (1.3×10^{-2} s^{-1}) than areas of divergence (1.2×10^{-2} s^{-1}). These results are consistent with the near symmetry of the roll circulation and suggest that the updraft portion of the roll circulation may be slightly stronger than the downdraft portion, consistent with theory [*Foster*, 2005]. Normal flow cases of rolls were most commonly found at an elevation angle of 2.4° and a range of about 5 km. This yielded a maximum residual observation height of about 210 m, which seems consistent with a height of about 200 m for the level of maximum residuals in the along-flow direction. The average wavelength of the transverse circulations of roll vortices was 1800 m. Although this is larger than the 1400 m average wavelength from the along-roll cases, the number is consistent with the theory that only the larger roll circulations will be observed by the radar using this method because the

Table 1. Comparisons of Physical Characteristics of Roll Vortices Found by This Study, by *Morrison et al.* [2005], and by *Foster* [2005][a]

	Ellis	*Morrison et al.* [2005]	*Foster* [2005]
Count	99	149	N/A
Wavelength (m)	1350	1450	1004
Depth (m)	730	660	500
Aspect ratio	2.1	2.4	2.4
Positive residual velocity (U) (m s^{-1})	6.5	7.0	2.2
Orientation (deg)	−2.0	−3.9	−3.5
Momentum flux[b] (m^2 s^{-2})	9.3	8.0	NA
Vorticity (s^{-1})	0.024	NA	NA
Updraft (m s^{-1})	2.75	NA	1.4
Downdraft (m s^{-1})	2.50	NA	1.1

[a]Aspect ratio is the result of the wavelength divided by the depth. Orientation is with respect to the direction of the average velocity. NA, not available.

[b]Momentum flux is calculated using an areal average.

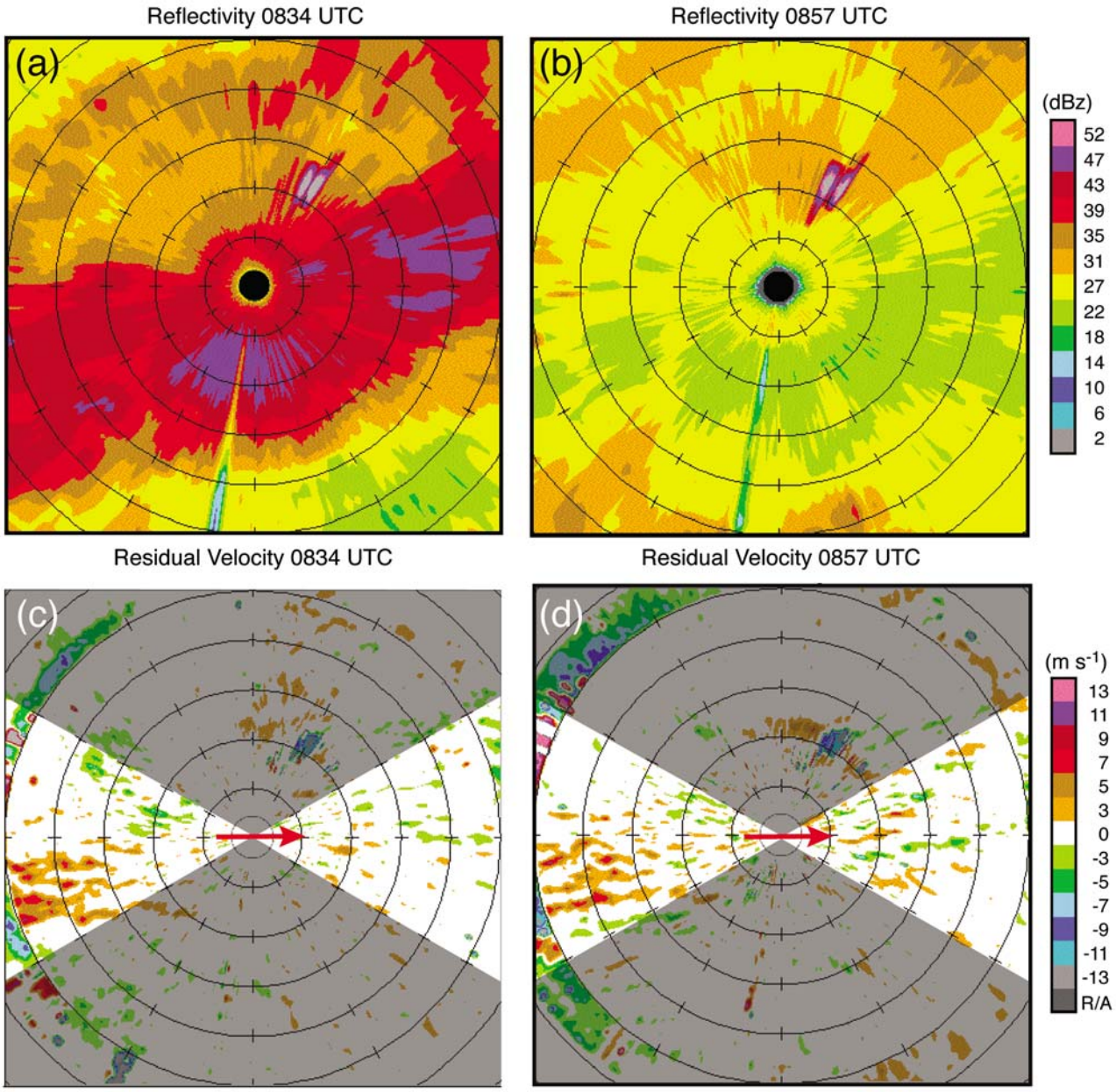

Figure 13. Examples of (a and b) reflectivity and (c and d) residual velocity for rainband (Figures 13a and 13c) and postrainband (Figures 13b and 13d) scans in Typhoon Keith. Range rings are 2 km apart.

cross-roll residual velocities tend to be smaller than the along-roll residuals, causing the velocity threshold to mask the smaller circulations.

4. Conclusions

[38] The goal of this paper was to document roll vortices in the highly sheared rotating HBL winds of typhoons over the Pacific Ocean using data from the WSR-88D radar located on Guam. Doppler-radar-derived low-level winds during Typhoons Dale (1996) and Keith (1997) were analyzed for coherent structures. The results yielded the first observational analysis of roll vortices in tropical cyclones over the Pacific Ocean. In total, 99 cases of roll vortices were observed. A total of 678 PPI scans were examined with roll activity present in 312 of these scans, or about 46% of the time. Rolls were found to cover about 50% of the area scanned by the radar in nonconvective situations and about 10% of the area scanned in convective situations. Enhanced friction over Guam's complex terrain was found to reduce the occurrence of rolls by about 75% in Typhoon Keith.

[39] The results of this work support and extend the findings of *Morrison et al.* [2005] (Table 1). The locations of rolls within the tropical cyclone were explored and mapped relative to the storm center. Combining the results of this study and *Morrison et al.* [2005], rolls were observed in all four quadrants of tropical cyclones. Residual velocity maxima associated with roll vortices in this study were most frequently found at an elevation angle of 1.4° and a distance

of 3–6 km from the radar. This translates to a mean height of about 200 m above ground level.

[40] A typical boundary layer roll observed in the two typhoons studied here has a wavelength of about 1400 m and a depth of about 700 m, and an aspect ratio of about 2, or 2:1. Positive and negative horizontal velocity anomalies, associated with roll circulations, average about 7 m s^{-1} and the estimated areal-averaged momentum flux generated by a typical roll is 8–9 m^2 s^{-2}. This value increases to about 17 m^2 s^{-2} when considering momentum flux associated with the downdraft portion of the roll and about 20 m^2 s^{-2} with the roll updraft. On average, the orientation of the rolls is about 2° to the left of the mean wind and the vertical component of vorticity produced by rolls is of the order of 10^{-2} s^{-1}. Rolls updrafts were estimated to be about 2.1 m s^{-1} and downdrafts about −1.9 m s^{-1}. VAD profiles and a mixing length approach were used to infer that the depth of the average roll circulation was about 700 m.

[41] Evidence of transverse circulations associated with roll vortices was also documented by the WSR-88D in the direction perpendicular to the mean flow. As expected, the magnitude of these transverse residuals were smaller than the anomalies documented parallel to the mean flow, averaging about 5 m s^{-1} in Typhoon Keith. Convergence and divergence values associated with the transverse flow suggest that updrafts in rolls may be slightly larger than the downdrafts, consistent with theory [*Foster*, 2005].

5. Discussion

[42] The analysis approach taken in this research focuses on roll vortices that span the depth of the HBL. This approach is supported by theoretical and observational evidence that suggest that there are two categories of elongated helical circulations that have contrasting characteristics of scale and life cycle, and different underlying physical mechanisms: (1) streaks, which are short-lived shallow circulations that are the result of nonnormal mode-optimal perturbations and (2) roll vortices, which are longer-lived helical rolls that span the depth of the HBL and are the manifestation of normal mode or inflection-point instabilities of the sheared flow. The resolution of the WSR-88D radar data and the scale of the roll vortices allow the latter to be documented with some confidence.

[43] The results presented here are largely in agreement with those of *Morrison et al.* [2005]. Values of horizontal wind anomalies were very similar to those recorded in *Morrison et al.* [2005] (about 1 m s^{-1} slower; a difference that is not statistically significant). Roll orientation varied but, on average, tended to align slightly to the left of the mean wind. Combining results from *Morrison et al.* [2005] and this study suggests that roll vortices can occur in all four quadrants of tropical cyclones over the Atlantic as well as Pacific oceans, providing evidence that the formation of roll vortices in tropical cyclones is not basin dependent. Transverse circulations observed perpendicular to the mean flow by the WSR-88D provide additional evidence of the prevalence of rolls in the tropical cyclone boundary layer. The results of the analysis of transverse circulations are consistent with expectations given the structure of helical rolls. Greater depths and shorter wavelengths reveal slightly lower aspect ratios than of those given by *Morrison et al.* [2005]. This could be attributed to the fact that rolls in this study were found at larger radii from the storm center where the HBL tends to be deeper, extending the upper bound within which rolls form. However, these differences also fall within the variability found in the roll statistics and could be attributed to sample size.

[44] The larger-scale features that appear to dominate this study and that of *Morrison et al.* [2005] are consistent with the HBL equivalent of classical boundary layer roll vortices as shown by *Foster* [2005]. The differences between HBL rolls and their classical counterparts is primarily due to the fact that even though HBL rolls generate large surface buoyancy fluxes, shear still dominates the nonlinear instability that generates the equilibrium rolls. Classical rolls that are common in midlatitude PBLs usually occur when buoyancy strengthens and modifies the dynamic instability. This study along with *Morrison et al.* [2005] and *Foster* [2005] indicates that the very strong HBL rolls generate nonlocal and nongradient fluxes that are of comparable magnitude to that which would be estimated using standard turbulence parameterizations applied to the observed mean wind profiles.

[45] *Nolan* [2005] found 4–5 km-scale roll-like bands nearly parallel to the mean wind, but only in a region just outside the radius of maximum winds. These bear a striking resemblance to the 4–10 km bands observed by *Gall et al.* [1998]. These structures may represent a third, larger scale of linear organization in the HBL.

[46] The smaller-scale linear features observed in the research DOW and SMART radars form in the highest shear region near the surface and are a persistent feature of the HBL [*Wurman and Winslow*, 1998; *Wurman et al.*, 2006; *Lorsolo et al.*, 2008]. These studies suggest that it is rare to find scans that do not include these linear features. By design, this study did not analyze the smallest scale features seen nearest the radar in the raw Doppler velocity scans, representing a limitation of the research presented here. It is likely that the streaks were also present in Typhoons Keith and Dale and it seems reasonable to suggest that the roll vortices documented in this study could modulate the intensity of these smaller surface layer circulations, thus influencing the surface fluxes. In this study and that of *Morrison et al.* [2005] subkilometer rolls were documented and the theory of *Foster* [2005] predicts them in some cases. However, it seems reasonable to suggest that at least some of the smaller-scale structures in this study could be near-surface streaks. Recent studies by *Moeng and Sullivan* [1994], *Foster* [1997], Drobiniski and *Foster* [2003], *Drobinski et al.* [2004], *Hunt and Carlotti* [2001], and *Hogstrom et al.* [2002] discuss the ubiquity of similar streaks in the near-surface region of strongly sheared atmospheric boundary layers and their importance to the generation and maintenance of the surface stress. *Hogstrom et al.* [2002] conclude that these subkilometer streaks establish favorable conditions for smaller-scale upward ejections of relatively low-speed near-surface air and downward sweeps of higher-speed air from higher in the near-surface region. These ejections and sweeps are the dominant processes that maintain the surface stress and form preferentially in the upward and downward branches, respectively, of the overturning circulations associated with the streaks.

[47] Given the presence of helical roll circulations, momentum fluxes were estimated [*Morrison et al.*, 2005; *Stull* 1998]. The estimates are valid at the midpoint of the roll depth (about 350 m) where the vertical velocity is a maximum. Given the nature of the analysis, these estimates are rough and may overestimate the surface fluxes, which are calculated for the surface layer (<100 m). It has been suggested that the magnitude of the surface fluxes should increase downward, where increased cross-isobar flow contributes kinetic energy; however, this is a topic for future research [*Morrison et al.*, 2005]. While rare, individual cases in rolls showed upward and downward momentum fluxes upward of 50 $m^2 s^{-2}$. In contrast, *Zang et al.* [2008] show that HBL rolls increase the surface fluxes by a factor of only O(50%) for one leg of aircraft data. Momentum fluxes presented in this study are associated with the largest roll vortices in the HBL. It follows that fluxes averaged for all sizes of rolls, including streaks in the surface layer, could be significantly smaller than those reported here. A large eddy simulation conducted by *Zhu* [2008] analyzing a wide spectrum of large eddy circulations illustrates this point.

[48] *Foster* [2005] noted asymmetries in the analytical analysis between the updraft and downdraft portions of roll circulations. In the analytical solution, vertical velocities were about 1.4 m s^{-1} in the updrafts and about −1.1 m s^{-1} in the downdrafts (Table 1). The vertical velocities estimated in Dale and Keith also showed that the estimated updrafts were larger than the downdrafts. Estimated values in this study tended to be larger than those predicted by the analytical solution, as was the case of *Morrison et al.* [2005] (Table 1). Theoretical results from *Foster* [2005] showed an average roll to have a horizontal velocity anomaly of 2.2 m s^{-1}, wavelength of 1004 m, depth of 500 m, aspect ratio of 2.4, and orientation of 3.5° to the left of the mean wind direction. While his velocity anomaly results are weaker than observed in this study, *Foster* [2005] did note that roll strength could be greater than those generated by the assumed mean flow profile used in his idealized study.

[49] *French et al.* [2007] found little evidence for HBL rolls in their flight-level data, but they also noted that the criteria used to select the cases might have eliminated some isolated rolls, especially in the along-wind runs. The results of this study suggest that to correctly assess the area of tropical cyclones affected by rolls in radar data, the precipitation structures in the storm and the radar's surrounding terrain environment need to be taken into account. This research shows more rolls occurring over water than land, whereas prior studies have documented roll vortices over land. The abrupt change and surface roughness at Guam's coast combined with circulations induced by Guam's complex terrain are the likely explanations for this difference. Reflectivity data showed rainbands in Typhoon Keith, whose convective-scale circulations also suppressed roll occurrence, consistent with the observations of *Morrison et al.* [2005].

[50] The goal of this study was to document the nature and pervasiveness of roll vortices in the boundary layer of tropical cyclones over the Pacific Ocean. Limitations of the WSR-88D data used in this study and their limited sample of only two typhoons support the argument that more data need to be collected to comprehensively address the question of how the HBL roll vortices interact with streaks in the surface layer to modulate the surface fluxes. The results of this study confirm their prevalence in Pacific typhoons, and suggest that their impact should be parameterized, if not resolved explicitly in the boundary layer simulations of tropical cyclone forecast models.

[51] **Acknowledgments.** The authors thank Gary Barnes, Tom Schroeder, and Ralph Foster for their suggestions and comments regarding these results. This work was supported under contract from the United States Army Corps of Engineers (W912HZ-05-C-0036).

References

Black, P. G., et al. (2007), Air-sea exchange in hurricanes: Synthesis of observations from the coupled boundary layer air-sea transfer experiment, *Bull. Am. Meteorol. Soc.*, *88*, 357–374, doi:10.1175/BAMS-88-3-357.

Brown, R. A., and L. Zeng (2001), Comparison of planetary boundary layer model winds with dropsonde observations in tropical cyclones, *J. Appl. Meteorol.*, *40*, 1718–1723, doi:10.1175/1520-0450(2001)040<1718:COPBLM>2.0.CO;2.

Browning, K. A., and R. Wexler (1968), The determination of kinematic properties of a wind field using Doppler radar, *J. Appl. Meteorol.*, *7*, 105–113, doi:10.1175/1520-0450(1968)007<0105:TDOKPO>2.0.CO;2.

Carbone, R. E., M. J. Carpenter, and C. D. Burghart (1985), Doppler radar sampling limitations in convective storms, *J. Atmos. Oceanic Technol.*, *2*, 357–361, doi:10.1175/1520-0426(1985)002<0357:DRSLIC>2.0.CO;2.

Christian, T. W., and R. M. Wakimoto (1989), The relationship between radar reflectivities and clouds associated with horizontal roll convection on 8 August 1982, *Mon. Weather Rev.*, *117*, 1530–1544, doi:10.1175/1520-0493(1989)117<1530:TRBRRA>2.0.CO;2.

Crum, T. D., and R. L. Alberty (1993), The WSR-88D and the WSR-88D operational support facility, *Bull. Am. Meteorol. Soc.*, *74*, 1669–1687, doi:10.1175/1520-0477(1993)074<1669:TWATWO>2.0.CO;2.

Deardorff, J. W. (1972), Numerical investigation of neutral and unstable planetary boundary layers, *J. Atmos. Sci.*, *29*, 91–115.

Drobinski, P., and R. C. Foster (2003), On the origin of near-surface streaks in the neutrally stratified planetary boundary layer, *Boundary Layer Meteorol.*, *108*, 247–256, doi:10.1023/A:1024100125735.

Drobinski, P., P. Carlotti, R. K. Newsom, R. M. Banta, R. C. Foster, and J. L. Redelsperger (2004), The structure of the near-neutral atmospheric surface layer, *J. Atmos. Sci.*, *61*, 699–714, doi:10.1175/1520-0469(2004)061<0699:TSOTNA>2.0.CO;2.

Emanuel, K. A. (1986), An air-sea interaction theory for tropical cyclones. Part I: Steady-state maintenance, *J. Atmos. Sci.*, *43*, 585–605, doi:10.1175/1520-0469(1986)043<0585:AASITF>2.0.CO;2.

Emanuel, K. A. (1995), Sensitivity of tropical cyclones to surface exchange coefficients and a revised steady-state model incorporating eye dynamics, *J. Atmos. Sci.*, *52*, 3969–3976, doi:10.1175/1520-0469(1995)052<3969:SOTCTS>2.0.CO;2.

Etling, D., and R. A. Brown (1993), Roll vortices in the planetary boundary layer: A review, *Boundary Layer Meteorol.*, *65*, 215–248, doi:10.1007/BF00705527.

Foster, R. C. (2005), Why rolls are prevalent in the hurricane boundary layer, *J. Atmos. Sci.*, *62*, 2647–2661, doi:10.1175/JAS3475.1.

French, J. R., W. M. Drennan, J. A. Zhang, and P. G. Black (2007), Turbulent fluxes in the hurricane boundary layer. Part I: Momentum flux, *J. Atmos. Sci.*, *64*, 1089–1102, doi:10.1175/JAS3887.1.

Fujita, T. T. (1992), Damage survey of Hurricane Andrew in south Florida, *Storm Data*, *34*, 25–30.

Gall, R. T., J. Tuttle, and P. Hildebrand (1998), Small-scale spiral bands observed in hurricanes Andrew, Hugo, and Erin, *Mon. Weather Rev.*, *126*, 1749–1766, doi:10.1175/1520-0493(1998)126<1749:SSSBOI>2.0.CO;2.

Ginis, I., A. P. Khain, and E. Morozovsky (2004), Effects of large eddies on the structure of the marine boundary layer under strong wind conditions, *J. Atmos. Sci.*, *61*, 3049–3064, doi:10.1175/JAS-3342.1.

Glendening, J. W. (1996), Lineal eddy features under strong shear conditions, *J. Atmos. Sci.*, *53*, 3430–3449, doi:10.1175/1520-0469(1996)053<3430:LEFUSS>2.0.CO;2.

Hogstrom, U., J. C. R. Hunt, and A. S. Smedman (2002), Theory and measurements for turbulence spectra and variances in the atmospheric neutral surface layer, *Boundary Layer Meteorol.*, *103*, 101–124, doi:10.1023/A:1014579828712.

Hunt, J. C. R., and P. Carlotti (2001), Statistical structure at the wall of the high Reynolds number turbulent boundary layer, *Flow Turbul. Combust.*, *66*, 453–475, doi:10.1023/A:1013519021030.

Katsaros, K. B., P. W. Vachon, W. T. Liu, and P. G. Black (2002), Microwave remote sensing of tropical cyclones from space, *J. Oceanogr.*, *58*, 137–151, doi:10.1023/A:1015884903180.

Kelly, R. D. (1982), A single Doppler radar study of horizontal-roll convection in a lake effect snow storm, *J. Atmos. Sci.*, *39*, 1521–1531, doi:10.1175/1520-0469(1982)039<1521:ASDRSO>2.0.CO;2.

Khanna, S., and J. G. Brasseur (1998), Three-dimensional buoyancy- and shear-induced local structure of the atmospheric boundary layer, *J. Atmos. Sci.*, *55*, 710–743, doi:10.1175/1520-0469(1998)055<0710:TDBASI>2.0.CO;2.

Knupp, K. R., J. Walters, and M. Biggerstaff (2006), Doppler profiler and radar observations of boundary layer variability during the landfall of tropical storm Gabrielle, *J. Atmos. Sci.*, *63*, 234–251, doi:10.1175/JAS3608.1.

LeMone, M. A. (1973), The structure and dynamics of horizontal roll vortices in the planetary boundary layer, *J. Atmos. Sci.*, *30*, 1077–1091, doi:10.1175/1520-0469(1973)030<1077:TSADOH>2.0.CO;2.

Lin, C.-L., J. C. McWilliams, C.-H. Moeng, and P. P. Sullivan (1996), Coherent structures and dynamics in a neutrally stratified planetary boundary layer, *Phys. Fluids*, *8*, 2626–2639.

Lorsolo, S., J. L. Schroeder, P. Dodge, and F. Marks (2008), An observational study of hurricane boundary layer small-scale coherent structures, *Mon. Weather Rev.*, *136*, 2871–2893, doi:10.1175/2008MWR2273.1.

Marks, F., P. Dodge, and C. Sandin (1999), WSR-88D observations of hurricane atmospheric boundary layer structure at landfall (preprints), paper presented at 23rd Conference on Hurricanes and Tropical Meteorology, Am. Meteorol. Soc., Dallas, Tex.

Moeng, C.-H., and P. P. Sullivan (1994), A comparison of shear- and buoyancy driven planetary boundary layer flows, *J. Atmos. Sci.*, *51*, 999–1022, doi:10.1175/1520-0469(1994)051<0999:ACOSAB>2.0.CO;2.

Morrison, I., S. Businger, F. Marks, P. Dodge, and J. A. Businger (2005), An observational case for the prevalence of roll vortices in the hurricane boundary layer, *J. Atmos. Sci.*, *62*, 2662–2673, doi:10.1175/JAS3508.1.

Nolan, D. S. (2005), Instabilities in hurricane-like boundary layers, *Dyn. Atmos. Oceans*, *40*, 209–236, doi:10.1016/j.dynatmoce.2005.03.002.

Stull, R. B. (1988), *An Introduction to Boundary Layer Meteorology*, Kluwer Acad., Dordrecht, Netherlands, pp. 206–208.

Weckwerth, T. M., J. W. Wilson, R. M. Wakimoto, and N. A. Crook (1997), Horizontal convective rolls: Determining the environmental conditions supporting their existence and characteristics, *Mon. Weather Rev.*, *125*, 505–526, doi:10.1175/1520-0493(1997)125<0505:HCRDTE>2.0.CO;2.

Wurman, J., and J. Winslow (1998), Intense sub-kilometer boundary layer rolls in Hurricane Fran, *Science*, *280*, 555–557, doi:10.1126/science.280.5363.555.

Wurman, J., C. Alexander, P. Robinson, and F. Masters (2006), Preliminary comparison of DOW and in situ wind measurements in Hurricane Rita, paper presented at 27th Conference on Hurricane and Tropical Meteorology, Am. Meteorol. Soc., Monterey, Calif., 23–28 April.

Zhang, J., K. B. Katsaros, P. G. Black, S. Lehner, J. R. French, and W. M. Drennan (2008), Effects of roll vortices on turbulent fluxes in the hurricane boundary layer, *Boundary Layer Meteorol.*, *128*, 173–189, doi:10.1007/s10546-008-9281-2.

Zhu, P. (2008), Simulation and parameterization of the turbulent transport in the hurricane boundary layer by large eddies, *J. Geophys. Res.*, *113*, D17104, doi:10.1029/2007JD009643.

S. Businger and R. Ellis, University of Hawai'i at Mānoa, 2525 Correa Rd., HIG 350, Honolulu, HI 96822, USA. (businger@hawaii.edu; rtellis@hawaii.edu)